Expedited Experimental Simulation of High Burnup Microstructure of Advanced Ferritic/martensitic Steel Claddings for Sodium-cooled Fast Reactor

Myeongkyu Lee, Geon Kim, Jungsu Ahn, Sangjoon Ahn*
Department of Nuclear Engineering, Ulsan National Institute of Science and Technology (UNIST)
50, UNIST-gil, Ulsan, Republic of Korea, 44919
**Corresponding author:sjahn99@unist.ac.kr*

1. Introduction

Fast nuclear reactor core demands fuel claddings endure unprecedented level of radiation damage up to ~150 dpa, about three-fold of their counterparts in Gen-II thermal nuclear reactors [1]. Historically, Ferritic/Martensitic (F/M) steels have demonstrated superior radiation performance up to high burnup of ~20 at% in EBR-II [2]. In this regard, Korea Atomic Energy Research Institute (KAERI) has been developing a series of variant F/M steels, named FC-92, aiming its employment in Prototype Gen-IV Sodium-cooled Fast Reactor (PGSFR) by 2028 [3].

The investigation on radiation performance of FC-92 is ongoing mainly by utilizing research reactors in and outside of the Republic of Korea, such as HANARO in KAERI and BOR-60 in Russia. However, these in-core tests are exceedingly time-consuming due to low radiation damage rate (< ~20 dpa per year) and hence cost ineffective especially when using oversea facilities. This issue can be partly resolved, or at least mitigated, by utilizing heavy ion-beam accelerators that can rapidly accumulate radiation damage at rates around ~100 dpa per day.

This study presents experimentally simulated radiation-damage-induced microstructural evolution of FC-92B with corresponding computational simulation results obtained using the Stopping and Range of Ions in Matter (SRIM).

2. Experimental

2.1. Specimen preparation and ion-beam irradiation

As-received alloy plate of FC-92B from KAERI was sectioned into several (10 mm × 10 mm × 4 mm) size cuboid by electrical discharge machining. The sectioned specimen surface (to be irradiated) was flattened using SiC papers and polished with 0.25 μm diamond suspension. The prepared specimens were shipped to the Low Energy Ion-beam Facilities in Korea Multi-purpose Accelerator Complex (KOMAC) and irradiated with 60 keV helium ion-beam at fluence of 2.47×10^{18} ions/cm^2.

2.2. Characterization of irradiated specimen

From the irradiated side of the specimens, (8 μm × 5 μm × 100 nm) size TEM specimens were lifted-out by using focused ion beam (FIB, FEI Helios 450HP) and characterized using a high-resolution transmission electron microscope (HR-TEM, JEM-2100) equipped with a spherical aberration (Cs) corrector.

2.3. Computational simulation of Radiation damage

SRIM-estimated radiation damage and implanted helium ion distributions in the irradiated FC-92B specimen are shown in Fig. 1. The displacement threshold energy of the specimen was set up as 40 eV, a recommended figure for polycrystalline materials by ASTM. It is noteworthy that the peak radiation damage is ~200 dpa and only 16 h of ion-beam irradiation was cable of achieving such kind of significant radiation damage, which properly demonstrates the handiness of the methodology.

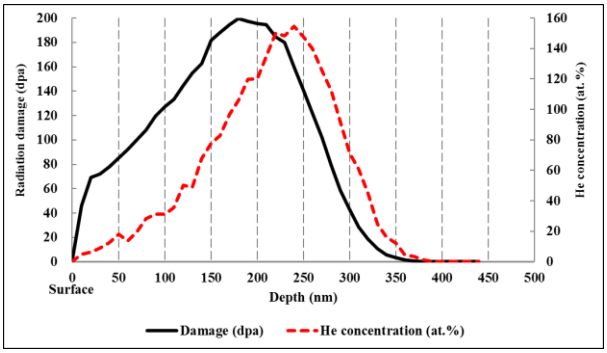

Fig. 1 Radiation damage and He distribution in FC-92B irradiated with 60 keV He+ ion-beam at the fluence of 2.47×10^{18} ions/cm^2 (SRIM-2013).

3. Results and discussion

Figure 2, a high-angle annular dark field (HAADF) image of the irradiated FC-92, shows clear distinction between the radiation-damaged area (dark, near surface) and unirradiated bulk of the alloy (bright, inner side) beyond penetration limit of implanted He ions in the alloy. The darker contrast of irradiated area indicates its porous characteristics compared with undamaged area. Vertical streaks are artifacts from the FIB procedure, since the patterns are more distinctively visible from the unirradiated area due to periodically uneven carving of the thicker part of specimen.

The inner (red-marked) layer of irradiated area enlarged in Fig. 3 are heavily damaged and shows isolated ellipsoidal (or near-spherical) smaller bubbles

and interconnected (irregular) large bubbles. Figure 4 shows Fe and Cr depletion corresponding to damaged regions. This extreme microstructural evolution was foresighted both quantitatively from the preliminary SRIM calculation and qualitatively from the upper limit burnup conditions for PGSFR adopted for the irradiation experiment. Also, the use of gaseous ions (He), instead of self-ion (Fe), for ion-beam irradiation was superintended to confirm the upper bound of this research assessing radiation performance of cladding materials for fast reactors under severe radiation environment. This damaged area was perhaps amorphized to a certain extent since the Selected Area Diffraction (SAD) pattern was very dim from the region.

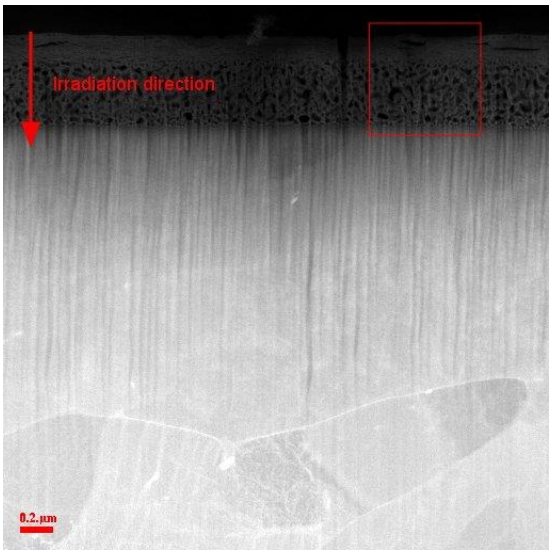

Fig. 2 High-angle annular dark field (HAADF) image of FC-92 steel irradiated with 60 keV He ion beam at the fluence of 2.47×10^{18} ions/cm^2.

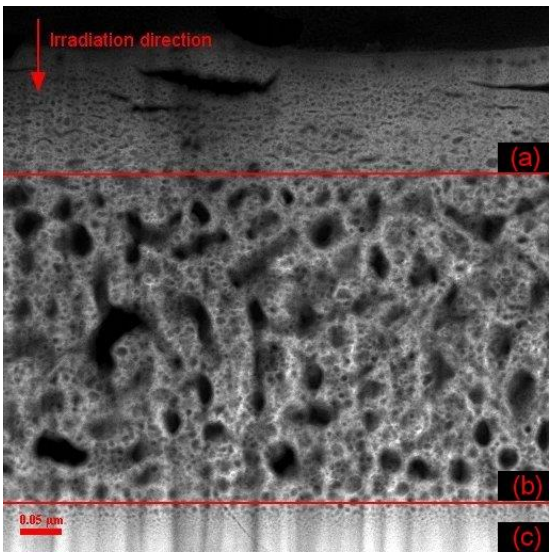

Fig. 3 Magnified radiation-damaged area from Fig. 2; (a) Low (< 180 dpa) damaged area (surface ~ 150 nm); (b) High (> 180 dpa) damaged area (150 nm ~ 550 nm); (c) Undamaged bulk (> 550 nm).

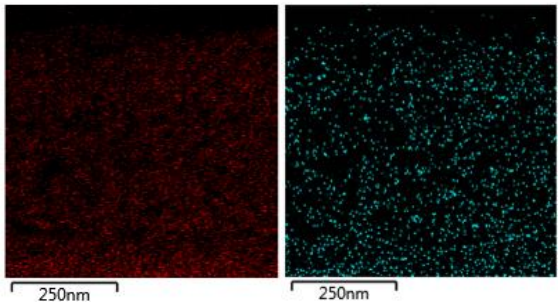

Fig. 4 Energy dispersive spectroscopy (EDS) results of porous radiation-damaged region shown in Fig. 3; (left) Fe K series; (right) Cr K series.

Void number density, average area, and areal fraction were measured from Fig. 3 using ImageJ 1.51f software. The void volume fraction was considered to correspond to void areal fraction.

Figure 5 shows the distribution of number density and area of voids and bubbles. Rapid decrease of void number density at ~150 nm reflects the active bubble coalescing above 180 dpa. Also negligibly small void area beyond ~600 nm confirms the practical penetration limits, which is ~200 nm deeper than the theoretical prediction shown in Fig. 1.

This broadening of radiation-damaged (or porous) layer (Fig. 6) was caused by in-situ decreasing of alloy density during irradiation, owing to void and bubble formation and growth from supersaturated vacancies. It is well known that vacancies remnant from radiation damage cascade and defect annihilation processes associating with local sink preferentially absorbing interstitials lead to the formation and growth of voids and bubbles [4, 5]. In other words, during the latter period of irradiation, effective density of the alloy was lower than the initial value used for the SRIM input deck. This sequential increase of penetration depth of He ions due to in-situ increasing of void volume fraction is computed using SRIM (Fig. 7). Note the penetration depth increase are consistent with the experimental results, since the calculated average penetration depth for ~35% void fraction alloy is ~320 nm, which is the center of porous layer shown in Fig. 3(b).

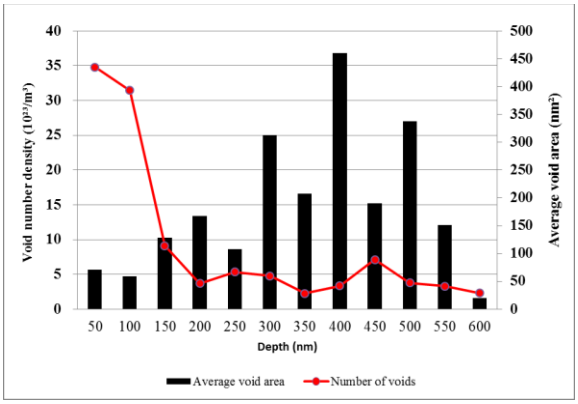

Fig. 5 Measured distribution of void number density and average void area from the irradiated FC-92 steel.

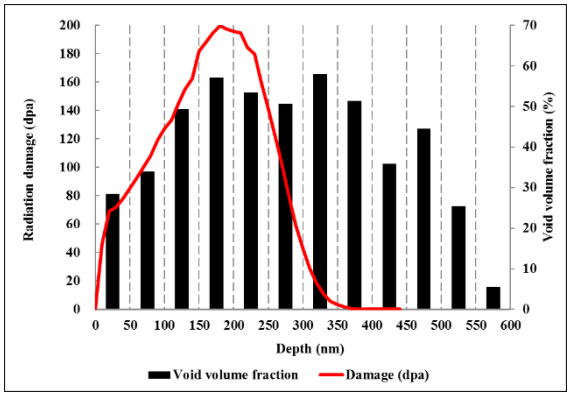

Fig. 6 Broadened peak of void volume fraction along penetration depth.

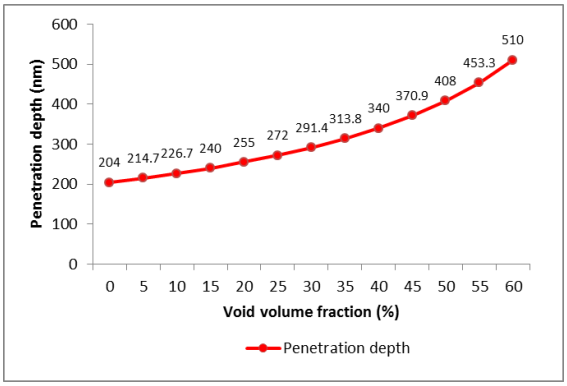

Fig. 7 Sequential increase of penetration depth of He ions into porous alloy

4. Conclusion

Prior to the full-scale assessment of radiation performance of FC-92, an F/M steel developed as PGSFR fuel cladding material, preliminary investigation on high burnup microstructural evolution of the cladding material was conducted utilizing ion-beam irradiation to be complementarily analyzed with in-pile test results.

The alloy irradiated using 60 keV He ion-beam at the fluence of 2.47×10^{18} ions/cm^2 exhibited approximately 400-nm wide highly radiation-damaged porous layer, embracing numerous voids and bubbles. The observed thickness of damaged area was ~200 nm thicker than initial SRIM prediction, which was modified by accounting for in-situ lowered effective density of alloy and showed a consistent match between measured void fraction of ~41% and peak damage location at ~ 350 nm.

5. Acknowledgements

Heavy ion irradiation was performed using ion-beam facilities in KOMAC. F/M steel specimens were provided by KAERI. This research was supported by the National Research Foundation of Korea (NRF) grant funded by the Korean Government (MSIP: Ministry of Science, ICT and future Planning) (No. 2016M2BA9912471)

References

[1] S.J. Zinkle, J.T. Busby, Structural materials for fission & fusion energy, Materials Today, 12 (2009) 12-19.
[2] L.C. Walters, Thirty years of fuels and materials information from EBR-II, Journal of Nuclear Materials, 270 (1999) 39-48.
[3] Y. Kim, Status of SFR development in Korea, in: Proceedings of International Conference on Fast Reactors and Related Fuel Cycles: Safe Technologies and Sustainable Scenarios (FR13), 2013, pp. 4-7.
[4] V.I. Dubinko, P.N. Ostapchuk, V.V. Slezov, Theory of radiation-induced and thermal coarsening of the void ensemble in metals under irradiation, Journal of Nuclear Materials, 161 (1989) 239-260.
[5] P.N. Ostapchuk, Generalized formalism of the void coarsening in theory of the vacancy swelling of metals, Voprosy Atomnoj Nauki i Tekhniki Fizika Radiatsionnykh Povrezhdenij i Radiatsionnoe Materialovedenie, 45 (2012).